

# Resonant Periodic Orbits of Trans-Neptunian Objects

Thomas A. Kotoulas, John D. Hadjidemetriou  
*University of Thessaloniki, Department of Physics*  
*GR-540 06 Thessaloniki, Greece*

## Abstract.

We study two and three-dimensional resonant periodic orbits, using the model of the restricted three-body problem with the Sun and Neptune as primaries. The position and the stability character of the periodic orbits determine the structure of the phase space and this will provide useful information on the stability and long term evolution of trans-Neptunian objects. The circular planar model is used as the starting point. Families of periodic orbits are computed at the exterior resonances  $1/2$ ,  $2/3$  and  $3/4$  with Neptune and these are used as a guide to select the energy levels for the computation of the Poincaré maps, so that all basic resonances are included in the study. Using the circular planar model as the basic model, we extend our study to more realistic models by considering an elliptic orbit of Neptune and introducing the inclination of the orbit. Families of symmetric periodic orbits of the planar elliptic restricted three-body problem and the three-dimensional problem are found. All these orbits bifurcate from the families of periodic orbits of the planar circular problem. The stability of all orbits is studied. Although the resonant structure in the circular problem is similar for all resonances, the situation changes if the eccentricity of Neptune or the inclination of the orbit is taken into account. All these results are combined to explain why in some resonances there are many bodies and other resonances are empty.

**Keywords:** Trans-Neptunian objects - periodic orbits - bifurcation - resonances

## 1. Introduction

The interest in studying exterior resonances is continuously growing after the discovery of many objects at the edge of the Solar System, beyond the orbit of Neptune, called Edgeworth-Kuiper (E-K) belt objects or trans-Neptunian objects (TNO) (Jewitt et.al. 1998, Jewitt 1999, Jewitt and Luu 2000). A large population of TNO's exists at the  $2/3$  mean motion resonance with Neptune, few objects have been found close to the  $1/2$  resonance and the  $3/4$  resonance is almost empty.

There are several papers on the dynamics of the Edgeworth-Kuiper belt objects: Levison and Stern (1995) studied the stability of orbits at the  $2:3$  resonance using numerical integration. The work of Duncan *et al.* (1995) is also based on numerical integration. They explored the whole area between 30 and 50 AU with particular interest to  $3/4$  and  $2/3$  mean motion resonances with Neptune. Furthermore, Morbidelli *et al.* (1995) investigated the resonant structure of the E-K belt by both



© 2002 Kluwer Academic Publishers. Printed in the Netherlands.

analytic and numerical means. Using an averaged three-dimensional model that takes into account both Neptune's and Uranus' perturbations, they studied the basic mean motion resonances with Neptune up to 50 AU, as well as secular resonances. A more recent work is the one of Morbidelli (1997), who studied exclusively the dynamical structure of the  $2/3$  resonance through the evolution of proper elements and with focus on slowly diffusing orbits. Malhotra (1996) studied the dynamics of the major mean motion resonances with Neptune from the  $5/6$  (at 34 AU) up to the  $1/3$  resonance (at 62.6 AU). Her study was based on computing Poincaré surfaces of section of the planar circular restricted three-body problem near these resonances. A circular orbit for Neptune was also considered by Yu and Tremaine (1999), who studied the four-body problem Sun-Neptune-Pluto -  $2/3$  resonant E-K object, (called Plutino) and thus determined the effect of Pluto on the stability of the Plutinos' orbits. Gallardo and Ferraz-Mello (1998) studied also the dynamics of the  $2/3$  resonance in the E-K belt. Maran and Williams (2000) studied the dynamical evolution of bodies initially situated in the Uranus-Neptune region, to investigate whether some bodies could evolve to the E-K belt and thus populate this region. Nesvorný and Roig (2000) made a systematic study of the  $2/3$  resonance and compared the results to the observed resonant population. A review of the dynamical structure of the E-K belt and the origin of the Jupiter family of comets is made by Morbidelli (1999) and Jewitt (1999).

A major problem which arises is: why some resonances are populated with a large number of objects, while other resonances are almost empty? This is obviously related to the topology of the phase space at these resonances, so that in one resonance trapping is possible and in another resonance a diffusion mechanism is present, due to chaotic motion.

The best way to obtain the structure of the phase space is to find all the basic periodic orbits. We remark that a resonance is associated to a periodic orbit. It is known that the periodic orbits, or equivalently, the fixed points on a Poincaré map, determine critically the topology of the phase space. For this reason we compute families of periodic orbits and study their stability.

We start our study with the circular planar three body problem. Although the nonzero eccentricity of Neptune and the inclination of the orbit of the small body play an important role in the evolution of the system, because they introduce one more degree of freedom, the circular planar case is the basic framework in the study of this problem. This is so because, starting from the circular planar case, it is easy to understand the more complicated structure of the more

realistic models, i.e. the elliptic and 3-D case and see in a clear way the differences between the various resonances.

Malhotra (1996) has made a detailed study of the phase space beyond the orbit of Neptune, in the framework of the restricted planar and circular three body problem. Several resonances are included in this study. In the present paper we extend the study to include a non-zero eccentricity of Neptune and we also consider 3-D orbits. As we shall see, it is in these, more realistic, models that the differences between the various resonances appear. We start by finding families of symmetric periodic orbits of the planar circular three-body problem at the  $1/2$ ,  $2/3$  and  $3/4$  mean motion resonances with Neptune. Several Poincaré maps are obtained in order to have a full description of the phase space. Using these families as the basic framework, we extend our study to more realistic models, elliptic and 3-D. The families of the elliptic problem bifurcate from the planar circular families at those points where the period is a multiple of the period of Neptune (in the inertial frame). The three dimensional families of symmetric periodic orbits bifurcate from the vertical critical orbits of the corresponding planar circular problem. Finally we study the stability of these orbits and we draw conclusions about the motion of TNO's at the above resonances with Neptune.

## 2. Families of periodic orbits of the circular planar problem

We assume that the orbit of Neptune is circular and we consider a rotating frame of reference  $Oxyz$  whose  $x$ -axis is the line joining the Sun,  $S$ , with Neptune,  $N$ , the positive direction being from  $S$  to  $N$ , its origin is at their centre of mass, the  $y$ -axis is in the orbital plane of Neptune and the  $z$ -axis is perpendicular to the  $xy$  plane. In the usual normalized units where the radius  $SN = 1$ , the gravitational constant is  $G = 1$  and the total mass  $m_S + m_N = 1$ , the differential equations of motion are the equations of the restricted circular 3-body problem (Roy, 1982).

In the rotating frame  $xOy$  there exist planar families of symmetric periodic orbits for the small object, which lie outside the orbit of Neptune and are nearly circular (generated by the continuation of circular Keplerian orbits around Sun when  $\mu = 0$ , by increasing the mass) or nearly elliptic (generated by the continuation of elliptic Keplerian orbits around Sun when  $\mu = 0$ ). All these orbits are symmetric periodic orbits with respect to the rotating  $x$ -axis.

A *simple* symmetric periodic orbit starts at  $t=0$  perpendicularly from the  $x$ -axis ( $y(0) = 0$ ,  $\dot{x}(0) = 0$ ) and crosses again perpendicularly

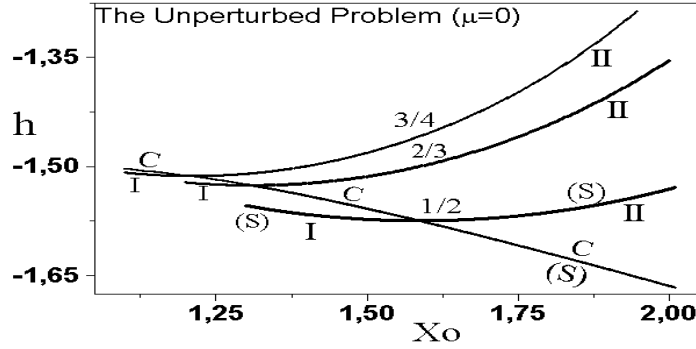


Figure 1. The characteristic curves of the unperturbed ( $\mu = 0$ ) families of periodic orbits. The curve  $C$  represents the family of circular orbits and along this family the semimajor axis  $a$ , or the ratio  $n/n'$ , varies. At the resonant values  $n/n' = 1/2, 2/3, 3/4$  we have a bifurcation of families of elliptic periodic orbits, along which the semimajor axis  $a$  and the ratio  $n/n'$  is constant and the eccentricity increases, starting with zero values.

the  $x$ -axis at the first intersection ( $y(T/2) = 0, \dot{x}(T/2) = 0$ ), where  $T$  is the period of the orbit. We call  $r$ -multiple periodic orbit a symmetric periodic orbit for which the first perpendicular crossing is at the  $r^{\text{th}}$  intersection with the  $x$ -axis (in the same direction). In this latter case  $r$  is the *multiplicity* of the periodic orbit. Since for a symmetric periodic orbit we have  $y(0) = 0, \dot{x}(0) = 0$ , the initial conditions are  $x(0)$  and  $\dot{y}(0)$ . Consequently, a symmetric periodic orbit can be represented by a point in the plane  $x_0 - \dot{y}_0$ , or equivalently, by a point in the plane  $x_0 - h$ , where  $h$  is the *Jacobi-constant*. Also, a monoparametric family of symmetric periodic orbits is represented by a smooth curve in the plane  $x_0 - h$ , which is called the "*characteristic curve*".

In the following we shall consider direct periodic orbits for the small object, i.e. the TNO revolves around the Sun in the same direction as that of Neptune (with respect to the inertial frame). For the normalized value of the mass of Neptune we have taken  $\mu = 5.178 \times 10^{-5}$ . The orbital period of Neptune around the Sun, in the normalized units we use, is equal to  $2\pi$ . We restrict our study to symmetric periodic orbits. From the numerical results that we have, we do not find any evidence for the existence of non-symmetric periodic orbits in the Edgeworth-Kuiper belt, at least for the major resonances.

In order to obtain a clear view of the resonant structure of the planar problem, for the Sun-Neptune mass ratio, we start with the unperturbed problem: Neptune, with zero mass, revolves around the Sun in a circular orbit and we study the motion of a massless body in the

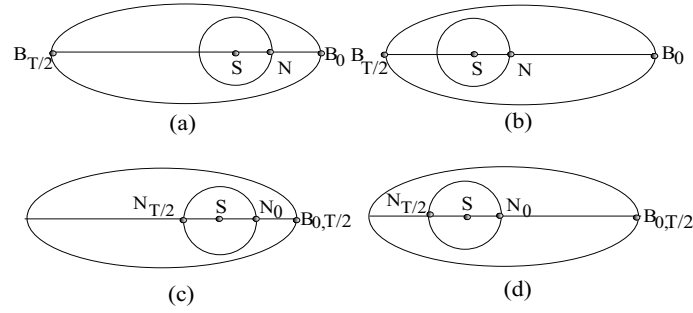


Figure 2. Resonances 1/2 and 3/4. Geometric configuration at  $t = 0$  and  $t = T/2$ : (a) family I,  $\sigma = 0$  (b) family II,  $\sigma = \pi$ . Resonance 2/3. Geometric configuration at  $t = 0$  and  $t = T/2$ : (c) family I,  $\sigma = 0$  and (d) family II,  $\sigma = \pi$ .

rotating frame  $xOy$  mentioned above. In Figure 1 we present the unperturbed family of circular periodic orbits (the small body in the Kuiper belt describes a *circular* orbit around the Sun) and the unperturbed families of symmetric elliptic periodic orbits (the small body describes an *elliptic* orbit around the Sun). These latter families bifurcate from the circular family at the resonant orbits  $n/n' = 1/2, 2/3, 3/4, \dots$ , where  $n$  is the mean motion of the small body and  $n'$  that of Neptune (in our normalized units  $n' = 1$ ).

Along an unperturbed family of elliptic periodic orbits the ratio  $n/n'$  is constant, equal to the corresponding ratio of the circular orbit from which this family bifurcates, but the eccentricity increases as we go “outwards”. We note that in each resonance there exist two different branches of the resonant family, differing in phase only, defined as *type I* and *type II*. These are shown in Figure 1. Also, a simple geometry gives the following configurations at  $t = 0$  and  $t = T/2$  for each resonance:

$$\underline{n/n' = 1/2 \text{ and } n/n' = 3/4 [(2\nu - 1)/2\nu]}$$

- (i) type I: at  $t = 0$ ,  $S - N - B_p$  ( $x_0 > 0$ ), at  $t = T/2$ ,  $B_a - S - N$  ( $x_0 < 0$ )
- (ii) type II: at  $t = 0$ ,  $S - N - B_a$  ( $x_0 > 0$ ), at  $t = T/2$ ,  $B_p - S - N$  ( $x_0 < 0$ )

$$\underline{n/n' = 2/3 [2\nu/(2\nu + 1)]}$$

- (i) type I: at  $t = 0$ ,  $S - N - B_p$  ( $x_0 > 0$ ), at  $t = T/2$ ,  $B_p - S - N$  ( $x_0 < 0$ )
- (ii) type II: at  $t = 0$ ,  $S - N - B_a$  ( $x_0 > 0$ ), at  $t = T/2$ ,  $B_a - S - N$  ( $x_0 < 0$ )

where  $S$ : Sun,  $N$ : Neptune and  $B$ : the small body in the Kuiper belt ( $B_a$  denotes position at aphelion and  $B_p$  position at perihelion). The geometry of this configuration is shown in Figure 2. Note that the geometry at  $t = 0$  and  $t = T/2$  for a  $p/q$  resonance depends on which  $p$  or  $q$  is even or odd.

The unperturbed families of periodic orbits described above can be continued to  $\mu > 0$ . The continuation of the circular orbits of the small body is possible in all cases except at the resonances of first order ( $n/n' = 1/2, 2/3, 3/4$ ). A review on the existence proofs is given in Hadjidemetriou (1988). In all other cases these orbits are continued as periodic orbits with a nearly circular orbit of the small body, called *periodic orbits of first kind*. The continuation of the elliptic families is also possible in all cases and we have, for  $\mu \neq 0$ , symmetric periodic orbits with nearly elliptic orbits of the small body, called *periodic orbits of second kind*. For each resonance we have two branches of resonant periodic orbits, branch  $I$  and branch  $II$  which differ in phase.

As we mentioned before, the continuation of the family of the circular orbits is not possible at the resonances  $1/2, 2/3$  and  $3/4$  with Neptune. The unperturbed family of circular orbits breaks down at this point and a gap appears close to the corresponding resonance. This is shown in Figures 3a, 4a, 5a. As we see, one part of the circular family is connected with the branch  $I$  of the resonant elliptic orbits and the other part of the circular family is connected with the branch  $II$  of elliptic orbits. The symbols “S” and “U” denote stability or instability, respectively.

resonance  $1/2$ : Family  $I_{1/2}$  is unstable and family  $II_{1/2}$  starts as stable until a value of eccentricity up to  $e = 0.035$  ( $x_0 = 1.644$ ) and then becomes unstable. At a very high value of eccentricity ( $e = 0.96$ ) the family  $II_{1/2}$  becomes again stable (Figure 3a).

resonance  $2/3$ : Family  $I_{2/3}$  is unstable and family  $II_{2/3}$  is stable (Figure 4a).

resonance  $3/4$ : Also, family  $I_{3/4}$  is unstable and family  $II_{3/4}$  is stable (Figure 5a).

We have used in Figures 3a, 4a, 5a the Jacobi-constant ( $h$ ), instead of  $\dot{y}_0$ , for the vertical axis. The families of periodic orbits of Figures 3a, 4a, 5a are very useful, because they provide a guide as where to take the energy levels for the Poincaré map, and which resonances to expect at each level. The corresponding energy levels for which we computed the Poincaré maps (Figure 12) are indicated at these figures. In this way we can readily see what fixed points will appear, which is the corresponding resonance and what is their stability.

In Figures 3b, 4b and 5b we present the periodic orbits at the  $1/2, 2/3$  and  $3/4$  resonances, in the axes resonance-eccentricity. In these

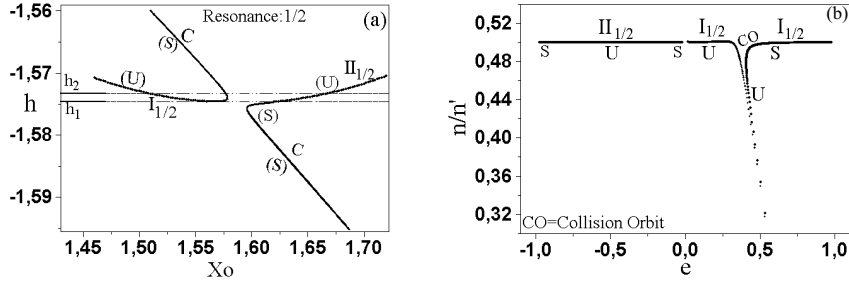


Figure 3. (a) The families of periodic orbits of the first and second kind near the  $1/2$  resonance, (b) The families of periodic orbits of the second kind near the  $1/2$  resonance for  $\mu > 0$  in a diagram  $n/n'$  - eccentricity. The gap at the corresponding resonance, due to the non-continuation of the circular orbits, is clearly seen close to  $e = 0$ . One more gap appears on  $I_{1/2}$  due to a collision orbit.

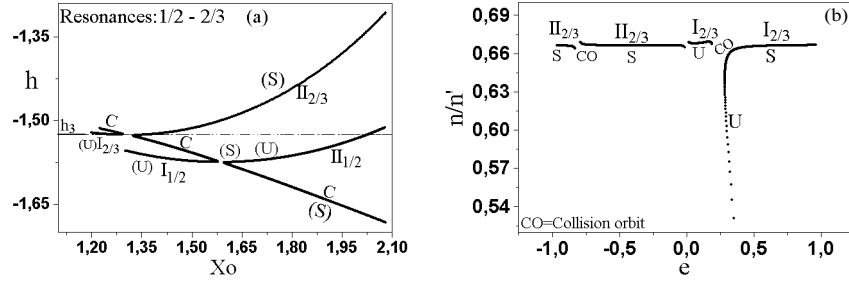


Figure 4. (a) The families of periodic orbits of the first and second kind near the  $1/2$  and  $2/3$  resonances, (b) The families of periodic orbits of second kind near the  $2/3$  resonance with Neptune for  $\mu > 0$ . The symbols "S" and "U" denote for stability and instability respectively. The gaps at the above resonances, due to the non-continuation of the circular orbits, is clearly seen in Figure 4a, close to  $e = 0$ . Two more gaps appears on  $I_{2/3}$  and on  $II_{2/3}$  due to a collision orbit.

diagrams,  $e > 0$  denotes position at perihelion and  $e < 0$  position at aphelion. The resonant elliptic orbits, along which the eccentricity increases and the gaps, separating the families  $I$  and  $II$  at  $e = 0$ , are clearly seen. Another feature on the resonant elliptic families  $I_{p/q}$  and  $II_{p/q}$  ( $p/q = 1/2, 2/3, 3/4$ ) is the appearance of collision orbits at  $e \neq 0$ .

A simple geometry shows that along the families of type  $I_{p/q}$  ( $\sigma = 0$ ,  $\omega = 0$  at  $t = 0$ ), where at  $t = 0$  the small body is at perihelion, we have a collision orbit with Neptune when the eccentricity satisfies the relation  $a(1-e) = 1$ , where  $a$  is the semimajor axis of the corresponding resonant orbit. These collision orbits are at  $e = 0.37$  for  $n/n' = 1/2$ ,  $e = 0.24$  for  $n/n' = 2/3$  and  $e = 0.17$  for  $n/n' = 3/4$  (Figures 3b, 4b, 5b). The existence of the collision orbits has an effect on the stability of the periodic orbits of a family  $I_{p/q}$ . Thus, the family  $I_{1/2}$  is unstable

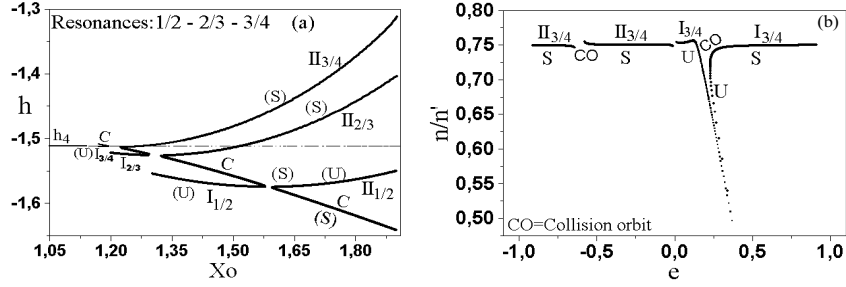


Figure 5. (a) The families of periodic orbits of the first and second kind near the 1/2, 2/3 and 3/4 resonances, (b) The families of periodic orbits of second kind near the 3/4 resonance with Neptune (for  $\mu > 0$ ). The symbols "S" and "U" denote for stability and instability respectively. The gaps at the above resonances, due to the non-continuation of the circular orbits, is clearly seen at  $e = 0$ . Two more gaps appear on  $I_{3/4}$  and on  $II_{3/4}$  due to a collision orbit.

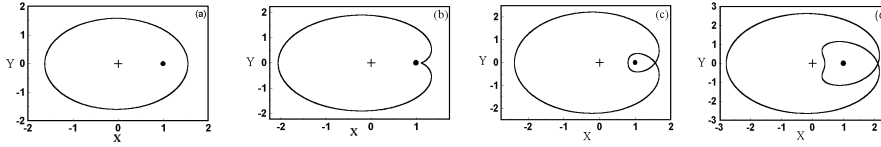


Figure 6. Periodic orbits along the family  $I_{1/2}$  (a)  $e=0.027$ , U (b)  $e=0.30$ , U (close to collision), (c)  $e=0.50$ , S and (d)  $e=0.75$ , S. Note the evolution of a collision orbit and the change of multiplicity from 1 to 2 as the eccentricity increases.

up to  $e = 0.41$  and then becomes stable. The multiplicity changes from 1 to 2 at  $e = 0.31$  (before the collision orbit) and then remains the same, equal to 2. The family  $I_{2/3}$  is unstable up to  $e = 0.29$  and then becomes stable. The multiplicity changes from 1 to 3 at  $e = 0.28$  (after the collision orbit) and then remains equal to 3. The family  $I_{3/4}$  is unstable up to  $e = 0.24$  and then becomes stable. The multiplicity changes from 1 to 2 at  $e = 0.14$  (before the collision orbit) and then changes again from 2 to 4 at  $e = 0.61$ . No other collision orbits exist along the families  $I_{1/2}$ ,  $I_{2/3}$  and  $I_{3/4}$ .

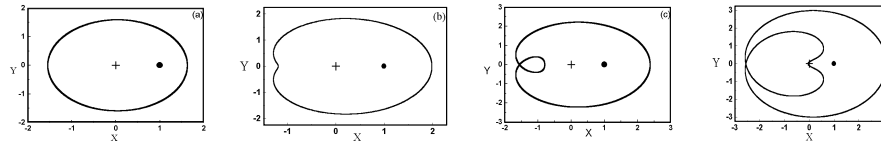


Figure 7. Periodic orbits along the family  $II_{1/2}$  (a)  $e=0.025$ , S (b)  $e=0.25$ , U (c)  $e=0.50$ , U and (d)  $e=0.965$ , S. Note the change of multiplicity from 1 to 2 as the eccentricity increases. No collision orbit with Neptune exists on this branch.

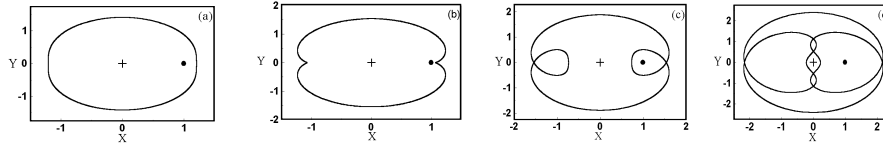


Figure 8. Resonance: 2/3 - Family  $I_{2/3}$  (a)  $e=0.08$ , U (b)  $e=0.18$ , U (close to collision), (c)  $e=0.44$ , S and (d)  $e=0.83$ , S. Note the change of the multiplicity from 1 to 3 after the collision, as the eccentricity increases.

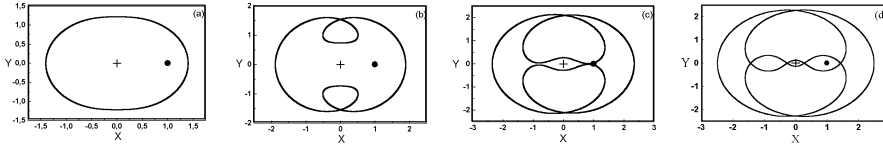


Figure 9. Resonance: 2/3 - Family  $II_{2/3}$  (a)  $e=0.07$ , S (b)  $e=0.44$ , S (c)  $e=0.791$ , U (close to collision) and (d)  $e=0.901$ , S. The development of a non-perpendicular collision orbit and the change of the multiplicity from 1 to 5 is clearly seen.

Along the resonant families of type  $II_{p/q}$  ( $\sigma = \pi$ ,  $\omega = \pi$  at  $t = 0$ ) we start with multiplicity  $r = 1$  but the multiplicity changes after a certain value of the eccentricity. More precisely, for the family  $II_{1/2}$  the multiplicity changes from 1 to 2 at  $e = 0.312$ . No collision orbits exist along the family  $II_{1/2}$ . Along the family  $II_{2/3}$  the multiplicity starts equal to 1 until  $e = 0.80$ , where a collision with Neptune occurs. At this point the multiplicity changes from 1 to 5. Along the family  $II_{3/4}$  the multiplicity changes from 1 to 2 at  $e=0.14$ . After this point, a collision occurs at  $e = 0.60$  and the multiplicity changes from 2 to 4. It changes again from 4 to 6 at a large value of eccentricity ( $e = 0.914$ ). The change of multiplicity along the families as the eccentricity increases, is due to geometric reasons, because we study the periodic orbit in a rotating frame.

The collision orbits along the families  $I_{1/2}$ ,  $I_{2/3}$  and  $I_{3/4}$  that we mentioned before, are perpendicular collisions, i.e. the small body crosses perpendicularly the  $x$ -axis during the collision. We also have collision orbits with Neptune on the resonant families of type  $II_{p/q}$ , namely  $II_{2/3}$  and  $II_{3/4}$ . These correspond to non perpendicular crossing of the  $x$ -axis during the collision. The evolution of the periodic orbits along the resonant families  $I_{p/q}$  and  $II_{p/q}$ , in the rotating frame, the change of the multiplicity as the eccentricity increases and the appearance of collision orbits is shown in Figures 6-11. The symbols (+) and (•) denote the position of the Sun and Neptune, respectively, on the rotating  $x$ -axis.

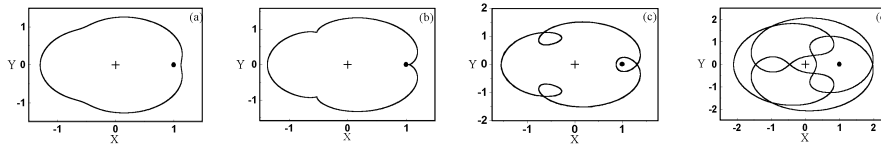


Figure 10. Periodic orbits along the family  $I_{3/4}$  (a)  $e=0.07$ , U (b)  $e=0.134$ , U (close to collision), (c)  $e=0.287$ , S and (d)  $e=0.734$ , S. Note the evolution of a collision orbit and the change of the multiplicity from 1 to 2 and from 2 to 4 for higher eccentricities.

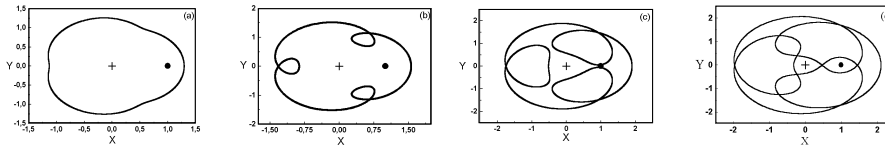


Figure 11. Periodic orbits along the family  $II_{3/4}$ : (a)  $e=0.07$ , S (b)  $e=0.286$ , S (c)  $e=0.574$ , U (close to collision) and (d)  $e=0.733$ , S. The development of a non-perpendicular collision orbit and the change of the multiplicity from 1 to 2 and from 2 to 4 is clearly seen.

### 3. The method of surface of section

For systems with two degrees of freedom a very useful numerical tool is the computation of the Poincaré mapping on a surface of section (for the details see Hénon, 1983, Lichtenberg and Leibermann, 1983). In the rotating  $xOy$  frame of reference, a convenient way to define the surface of section is to take  $y = 0$  and  $h = h_0$ , where  $h$  is the energy (Jacobi) constant and  $h_0$  the energy level at which we take the mapping. The Poincaré mapping is two dimensional, in the space  $x \dot{x}$  and defines the topology of the phase space on the surface of section. The consecutive points of the mapping may lie on a smooth curve, called *invariant curve*, if we are in an ordered region of phase space, or may be scattered if we are in a chaotic region. In many cases the distinction between these two extreme cases is sharp, but in some other cases the difference may not be clear.

An important feature of the mapping is the existence of *fixed points*. These correspond to the periodic orbits of the system and their position and stability characteristics determine critically the topology of the phase space. This makes clear the importance of the knowledge of the families of periodic orbits in the study of the problem.

In Figures 12a-d we present several Poincaré maps at the energy levels  $h_1$ ,  $h_2$ ,  $h_3$  and  $h_4$ , indicated in the Figures 3a, 4a and 5a. In this way we can readily see the relation of the fixed points of the map and the resonant periodic orbits.

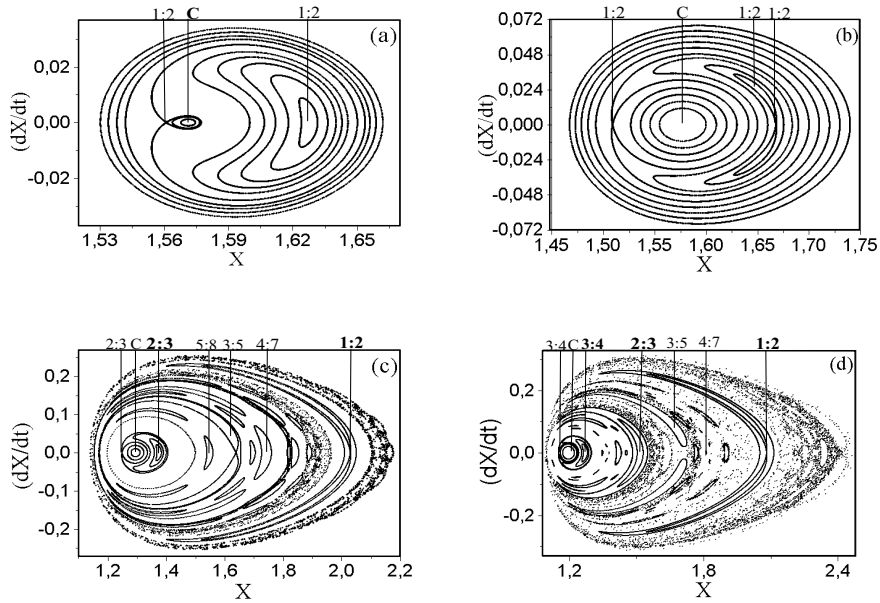


Figure 12. Poincaré maps at different energy levels: (a)  $h_1 = -1.574563$  ( $e = 0.02524$ ), (b)  $h_2 = -1.573304$  ( $e = 0.05057$ ), (c)  $h_3 = -1.524950$ , (d)  $h_4 = -1.512069$  of Figures 3a, 4a, 5a. The resonances at the corresponding fixed points are indicated. The circular fixed point is indicated by  $C$ . Note that for low energy levels namely (a) and (b), only the  $1/2$  resonance appears. The eccentricities in (a) and (b) are at the  $1/2$  resonance. As the energy  $h$  increases, more resonances appear and their overlap results to chaotic motion, which is stronger at higher energy levels.

In Figure 12a we present the Poincaré map at the energy level  $h_1 = -1.574563$  (Figure 3a). We note that there exist three basic fixed points: a stable fixed point, which corresponds to the  $1/2$  stable resonant elliptic periodic orbit of the family  $II_{1/2}$ , an unstable fixed point which corresponds to an  $1/2$  unstable resonant elliptic periodic orbit of the family  $I_{1/2}$ , and one more stable fixed point, denoted by  $C$  in Figure 12a, which is the closest fixed point to the circular part of the family. The stability region around this fixed point is very small, because the fixed point on the branch  $I_{1/2}$ , which is close to it, is unstable (Figure 3a). Only symmetric librations are found here, around the stable resonant fixed point. One *separatrix* is present. As we go "outwards" there exist only closed invariant curves which surround the *separatrix*. The phase space is regular in this case.

In Figure 12b we present the surface of section at a higher value of the energy,  $h_2 = -1.573304$  (Figure 3a). We observe that the topology of the phase space is different from that of Figure 12a. In place of the stable fixed point (corresponding to family  $II_{1/2}$ ) we have an unstable

fixed point and a double stable fixed point. This latter double fixed point corresponds to a new  $1/2$  resonant stable family (not shown in Figure 3) which bifurcates from  $II_{1/2}$  at the critical point, where the stability of the family  $II_{1/2}$  changes from stable to unstable. The eccentricity of this critical point is  $e = 0.035$ . Two separatrices are present: one surrounds the asymmetric librations and the other separates the inner and the outer circulation region. As we go "outwards" there exist only smooth invariant curves and the phase space remains regular. The stable librations around the non resonant circular fixed point  $C$  are due to the stable periodic orbit on the circular branch of the family of the periodic orbits, as one can see from Figure 3a, energy level  $h_2$ . It is clear that no other important resonances exist at the energy levels  $h_1$  and  $h_2$ .

As the energy level of the Poincaré map increases, many more resonances appear, as can be seen in Figures 12c and 12d. The corresponding energy levels are shown in Figure 4a for the Figure 12c and in Figure 5a for the Figure 12d. The identification of all the major resonant fixed points with the periodic orbits is clearly seen. From Figures 3a, 4a, 5a we can see that as  $h$  increases, more and more fixed points appear on the Poincaré surface of section. Their overlap is the reason of the appearance of the chaotic zones. On the surface of section, apart from the basic first order resonances  $1/2$ ,  $2/3$  and  $3/4$ , several other higher order resonances appear. The corresponding stable and unstable fixed points are the intersection of the line  $h = h_0$  with the higher order resonant periodic orbits, which exist in Figures 4a, 5a (not shown in these figures).

In Figure 12c we present the surface of section at the energy level  $h_3 = -1.524950$  (Figure 4a). We note that apart from the two mean motion resonances  $2/3$  and  $1/2$ , several other high order resonances are present:  $n/n' = 2/3$  at  $e = 0.05$ ,  $n/n' = 3/5$  at  $e = 0.165$ ,  $n/n' = 4/7$  at  $e = 0.20$  and  $n/n' = 1/2$  at  $e = 0.278$ . These resonances appear in the region "between" the two main first order resonances. In this energy level, a chaotic zone appears around the  $1/2$  resonance.

In Figure 12d we present the surface of section at the energy level  $h_4 = -1.512069$  (Figure 5a). We note that in this case all three major resonances of first order,  $1/2$ ,  $2/3$ ,  $3/4$  appear. The corresponding eccentricities, at the center of the resonance are:  $e = 0.31$ ,  $e = 0.16$  and  $e = 0.05$ , respectively. In addition, several other higher order resonances appear, namely  $n/n' = 4/7$  at  $e = 0.25$ ,  $n/n' = 3/5$  at  $e = 0.22$ . Large chaotic zones appear at this energy level, due to the overlap of the several resonances.

All the results above are in agreement with those found by Malhotra (1996).

The number of fixed points on the Poincaré surface of section, corresponding to a certain resonant periodic orbit, depends on the multiplicity of the periodic orbit, i.e. the number of intersections with the  $x$ -axis (in the same direction, say  $\dot{y} > 0$ ). For a simple periodic orbit, with multiplicity  $r = 1$ , we have only one fixed point. As however the energy level increases, the fixed point corresponds to larger values of the eccentricity (see Figures 6 - 11) and the multiplicity changes. The resonant orbit is now represented by a multiple fixed point (a set of fixed points). This is seen in Figures 12c-d.

Closing this paragraph, we remark that the circular planar problem is the simplest model for the study of the resonant motion. In most cases it is not a realistic model, because important information is missing. The ellipticity of the orbit of Neptune introduces the time explicitly and this is, in a sense, equivalent to an increase of the degrees of freedom. The three-dimensional motion introduces one more degree of freedom. In both these cases new resonant periodic orbits appear, at the corresponding resonance we study, and this changes the topology of the phase space and consequently the evolution of the system (compared to what we obtain with the circular planar model). The existence, or nonexistence, of the new resonances that appear when we extend the circular planar model to the elliptic problem or to the 3-D model, or both, plays a crucial role for the topology of the phase space and consequently for the evolution of the system, as we shall see in the following.

#### 4. The planar elliptic restricted three-body problem

In this section we will study the resonant structure of the elliptic restricted three body problem. The corresponding periodic orbits will be considered in a rotating frame  $xOy$  with the origin  $O$  at the center of mass of the Sun-Neptune system and the positive  $x$ -axis along the line Sun-Neptune. The orbit of Neptune is considered to be an elliptic orbit with a fixed eccentricity  $e_N$ . The  $xOy$  frame is a non-uniformly rotating frame, where the angular velocity of rotation is a known function of the time and Neptune moves on the rotating  $x$ -axis according to Keplerian theory. We have an non autonomous Hamiltonian system with two degrees of freedom, that depends periodically on time, with period equal to  $2\pi$  (this is the period of the orbit of Neptune). The energy integral does not exist in this case. This means that the stability depends on two pairs of eigenvalues, instead of one in the circular case (in this latter case the second pair was always equal to  $+1$ ).

TABLE 1  
*Bifurcation from the 2-D circular to the 2-D elliptic problem*

Resonance	$a_{res}$ (in A.U.)	Period	Bifurcation Points
1/2	47.777	$4\pi$	$e = 0.070$
1/2	47.777	$4\pi$	$e = 0.637$
2/3	39.398	$6\pi$	$e = 0.469$
3/4	36.415	$8\pi$	$e = 0.329$

We shall study families of periodic orbits of the elliptic problem at the 1/2, 2/3 and 3/4 mean motion resonances with Neptune. For a fixed value of the eccentricity of Neptune the periodic orbits of the elliptic problem are isolated. We can define a family of periodic orbits if we consider the eccentricity of Neptune,  $e_N$ , as a parameter. These families bifurcate from the families of periodic orbits of the circular problem at those orbits whose period is *exactly equal to a multiple of  $2\pi$* . Note that the period along the unperturbed ( $\mu = 0$ ) families  $I_{1/2}$ ,  $I_{2/3}$ ,  $I_{3/4}$  and  $II_{1/2}$ ,  $II_{2/3}$ ,  $II_{3/4}$  is exactly equal to  $4\pi$ ,  $6\pi$  and  $8\pi$ , respectively, and the perturbation  $\mu > 0$  slightly changes this value. Whether on the perturbed families there exist orbits with period an *exact* multiple of  $2\pi$ , and at what eccentricity, depends on the particular family. From the numerical computations it turns out that there exist periodic orbits along the families  $II_{1/2}$ ,  $II_{2/3}$ ,  $II_{3/4}$  whose period is *exactly* equal to  $4\pi$ ,  $6\pi$  and  $8\pi$  respectively, shown in Table 1. No bifurcation points exist on the families  $I_{1/2}$ ,  $I_{2/3}$  and  $I_{3/4}$ . From each of the above orbits, there bifurcate two families of periodic orbits of the elliptic problem, with  $e_N$  as a parameter. We shall call these families  $E_p^{p/q}$  and  $E_a^{p/q}$  ( $p/q = 1/2, 2/3, 3/4$ ). On family  $E_p$  Neptune is at perihelion and on  $E_a$  Neptune is at aphelion, at  $t = 0$ . The geometric configuration of the families of type  $E_1$  and  $E_2$  is shown in Figure 13.

The periodic orbits of the elliptic problem that are known, are all symmetric with respect to the  $x$ -axis of the rotating frame. These orbits start perpendicularly from the  $x$ -axis and at the same time the velocity of Neptune on the  $x$ -axis is equal to zero (i.e. Neptune is either at aphelion or perihelion). In this case the initial conditions of a periodic orbit are given by:  $x_0, y_0 = 0, (dx/dt)_0 = 0, (dy/dt)_0$  (in the rotating frame) for each value of the eccentricity of Neptune ( $e_N$ ). We can represent a family of symmetric periodic orbits by a *characteristic curve* in the

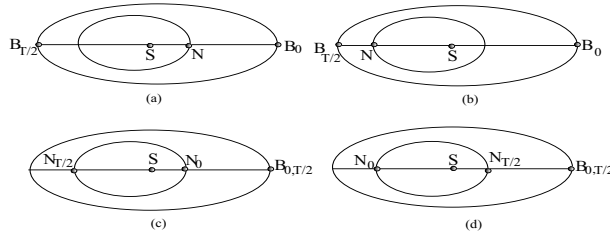


Figure 13. Elliptic problem - Geometric configuration at  $t = 0$  and  $t = T/2$ . Resonances 1/2 and 3/4: (a) family  $E_p$ ,  $\sigma = \pi, \nu = 0$  (b) family  $E_a$  ( $\sigma = \pi, \nu = \pi$ ). Resonance 2/3: (c) family  $E_p$ ,  $\sigma = \pi, \nu = 0$  (d) family  $E_a$  ( $\sigma = \pi, \nu = \pi$ ).

space  $x_0 - \dot{y}_0 - e_N$ , with an indication whether Neptune is at perihelion or aphelion.

The families of periodic orbits in the elliptic problem are with  $e_N$  as a parameter. So, for the present value of the eccentricity of Neptune,  $e_N = 0.011$ , we have a set of isolated pairs of periodic orbits.

### The 1/2 Resonance

There are two pairs of families of periodic orbits bifurcating from the planar orbits on the family  $II_{1/2}$ , at the eccentricities  $e = 0.07$  and  $e = 0.637$ , respectively. One pair is  $E_{1p}^{1/2}, E_{1a}^{1/2}$  and the other is  $E_{2p}^{1/2}, E_{2a}^{1/2}$ . Along the families  $E_{1p}^{1/2}, E_{2p}^{1/2}$  we have  $\sigma = \pi, \nu = 0$  and along the families  $E_{1a}^{1/2}, E_{2a}^{1/2}$  we have  $\sigma = \pi, \nu = \pi$ . The angles  $\sigma, \nu$  are defined as

$$\sigma = -\lambda' + 2\lambda - \varpi, \quad \nu = +\lambda' - 2\lambda + \varpi'$$

where  $\lambda$  is the mean longitude,  $\varpi$  the longitude of perihelion of the small body, and the primed quantities refer to Neptune.

The numerical computations revealed that the families  $E_{1a}^{1/2}$  and  $E_{2a}^{1/2}$  join in one family, at a maximum eccentricity at  $e_N = 0.24$ . These families are shown in Figure 14a. Both of them are unstable. The curves on the  $x_0, (dy/dt)_0$  plane are the two families of the circular problem that are given in Figure 3b.

### The 2/3 Resonance

There is one pair of families of periodic orbits bifurcating from the planar orbits on the family  $II_{2/3}$ , at the eccentricity  $e = 0.469$ . The pair is:  $E_p^{2/3}, E_a^{2/3}$ . Along the family  $E_p^{2/3}$ , we have  $\sigma = \pi, \nu = 0$  and along the family  $E_a^{2/3}$  we have  $\sigma = \pi, \nu = \pi$ . The angles  $\sigma, \nu$  are defined as

$$\sigma = -2\lambda' + 3\lambda - \varpi, \quad \nu = +2\lambda' - 3\lambda + \varpi'$$

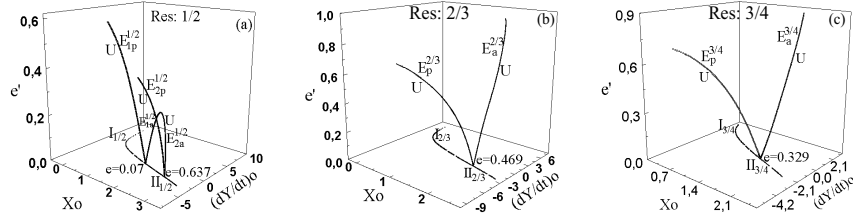


Figure 14. Families of periodic orbits of the elliptic restricted three-body problem at: (a) 1/2 resonance, (b) 2/3 resonance and (c) 3/4 resonance. The symbols “S”, “U” denote stability or instability, respectively.

These families are shown in Figure 14b. Both of them are unstable. The curves on the  $x_0, (dy/dt)_0$  plane are the two families of the circular problem that are given in Figure 4b.

### The 3/4 Resonance

There is one pair of families of periodic orbits bifurcating from the planar orbits on the family  $II_{3/4}$ , at the eccentricity  $e = 0.329$ . The pair is:  $E_p^{3/4}$ ,  $E_a^{3/4}$ . Along the family  $E_p^{3/4}$ , we have  $\sigma = \pi$ ,  $\nu = 0$  and along the family  $E_a^{3/4}$  we have  $\sigma = \pi$ ,  $\nu = \pi$ . The angles  $\sigma$ ,  $\nu$  are defined as

$$\sigma = -3\lambda' + 4\lambda - \varpi, \quad \nu = +3\lambda' - 4\lambda + \varpi'.$$

These families are shown in Figure 14c. Both of them are unstable. The curves on the  $x_0, (dy/dt)_0$  plane are the two families of the circular problem that are given in Figure 5b.

## 5. The 3-D restricted circular three-body problem

We present in this section resonant families of periodic orbits of the three dimensional circular restricted 3-body problem, at the resonances 1/2, 2/3 and 3/4. These families, if there exist, should bifurcate from the families of type  $I$  or  $II$  of the planar circular problem at those orbits whose stability is critical with respect to perturbations along the  $z$ -axis. For the computation of the vertical stability we used the method developed by Hénon (1973). The computations have revealed that the families  $I_{1/2}$ ,  $I_{2/3}$  and  $I_{3/4}$  are vertically stable; so, no 3-D periodic orbits can bifurcate from these families. Also, the families of circular orbits close to the resonances 1/2, 2/3 and 3/4 are vertically stable. So, simple 3D-bifurcations do not exist for the circular branch of the plane families (with  $\mu > 0$ ). On the other hand, vertical critical orbits do exist along the families  $II_{1/2}$ ,  $II_{2/3}$  and  $II_{3/4}$ . The results are

presented in Table 2. The families of the three-dimensional periodic orbits which bifurcate from these vertical critical orbits are described below.

TABLE 2  
*Bifurcation from the 2-D circular to the 3-D circular problem*

Resonance	$a_{res}$ (in A.U.)	Bifurcation Points
1/2	47.777	$e = 0.059$
1/2	47.777	$e = 0.066$
2/3	39.398	$e = 0.421$
2/3	39.398	$e = 0.450$
2/3	39.398	$e = 0.968$
3/4	36.415	$e = 0.291$
3/4	36.415	$e = 0.307$
3/4	36.415	$e = 0.663$
3/4	36.415	$e = 0.753$
3/4	36.415	$e = 0.767$

There are two types of three-dimensional symmetric periodic orbits on the rotating  $Oxyz$  frame:

*Type 1: Symmetric periodic orbits respect to the  $xz$ -plane.*

A 3-D simple symmetric periodic orbit starts at  $t = 0$  perpendicularly from the  $xz$ -plane ( $y(0) = 0$ ,  $\dot{x}(0) = 0$ ,  $\dot{z}(0) = 0$ ) and crosses again perpendicularly the  $xz$ -plane at the first intersection ( $y(T/2) = 0$ ,  $\dot{x}(T/2) = 0$ ,  $\dot{z}(T/2) = 0$ ), where  $T$  is the period of the orbit. For a multiple symmetric periodic orbit the first perpendicular crossing is at the  $r^{th}$  intersection with the  $xz$ -plane in the same direction, where  $r$  is the multiplicity of the periodic orbit. Since for a symmetric periodic orbit we have  $y(0) = 0$ ,  $\dot{x}(0) = 0$ ,  $\dot{z}(0) = 0$ , the non-zero initial conditions are:  $x(0)$ ,  $\dot{y}(0)$  and  $z(0)$ . Consequently, a symmetric periodic orbit can be represented by a point in the space  $x_0 - \dot{y}_0 - z_0$ , or because of the existence of the Jacobi integral, by a point in the space

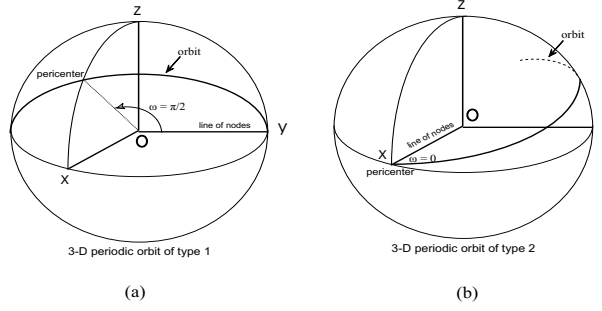


Figure 15. (a) The geometric configuration of a 3-D symmetric periodic orbit of *Type 1* ( $\omega = \pi/2$ ). (b) The geometric configuration of a 3-D symmetric periodic orbit of *Type 2* ( $\omega = \pi$ ).

$x_0 - h_0 - z_0$ , where  $h_0$  is the *Jacobi*-constant. Also, a monoparametric family of symmetric periodic orbits is represented by a smooth curve in the space  $x_0 - h_0 - z_0$ , which is called the “*characteristic curve*”. From the geometry of the orbit it can be seen that at  $t = 0$  the argument of pericenter is equal to  $\omega = \pi/2$  or  $\omega = 3\pi/2$  depending on whether the small body is at perihelion or aphelion (Figure 15a).

*Type 2: Symmetric periodic orbits respect to the x-axis.*

A 3-D simple symmetric periodic orbit starts at  $t = 0$  perpendicularly from the  $x$ -axis ( $y(0) = 0$ ,  $z(0) = 0$ ,  $\dot{x}(0) = 0$ ) and crosses again perpendicularly the  $x$ -axis at the first intersection ( $y(T/2) = 0$ ,  $z(T/2) = 0$ ,  $\dot{x}(T/2) = 0$ ), where  $T$  is the period of the orbit. For a multiple symmetric periodic orbit the first perpendicular crossing is at the  $r^{\text{th}}$  intersection with the  $x$ -axis, where  $r$  is the multiplicity of the periodic orbit. Due to the fact that for a symmetric periodic orbit we have  $y(0) = 0$ ,  $z(0) = 0$ ,  $\dot{x}(0) = 0$ , the non-zero initial conditions are:  $x(0)$ ,  $\dot{y}(0)$  and  $\dot{z}(0)$ . Consequently, a symmetric periodic orbit can be represented by a point in the space  $x_0 - \dot{y}_0 - \dot{z}_0$ . So, a monoparametric family of symmetric periodic orbits is represented by a smooth curve in the space  $x_0 - \dot{y}_0 - \dot{z}_0$ , which is called the “*characteristic curve*”. From the geometry of the orbit it can be seen that at  $t = 0$  the argument of pericenter is equal to  $\omega = 0$  or  $\omega = \pi$ , depending on whether the small body is at perihelion or aphelion, respectively (Figure 15b).

The resonant angles  $\sigma$  and  $\sigma_z$  are defined as

$$\sigma = -(p+q)\lambda' + p\lambda + q\varpi, \quad \sigma_z = -(p+q)\lambda' + p\lambda + q\Omega, \quad (1)$$

where  $\varpi$  is the longitude of perihelion of the small body and  $\Omega$  is the longitude of the ascending node. The  $1/2$  resonance corresponds

to  $p = 2$ ,  $q = -1$ , the 2/3 resonance to  $p = 3$ ,  $q = -1$  and the 3/4 resonance to  $p = 4$ ,  $q = -1$ . The argument of perihelion  $\omega = \varpi - \Omega$  is given by  $\omega = \sigma_z - \sigma$ . For the families of type 1 we have  $\sigma = \pi$ ,  $\sigma_z = \pi/2$ ,  $\omega = \pi/2, 3\pi/2$  and  $\Omega = \pi/2$  and for the families of type 2 we have  $\sigma = \pi$ ,  $\sigma_z = 0$ ,  $\omega = 0, \pi$  and  $\Omega = 0$ . The inclination  $i$  can be computed from the initial conditions from the equation  $\cos i = L_z/L$ , where  $L$  is the angular momentum.

We shall present here the families of 3-D resonant periodic orbits at the 1/2, 2/3 and 3/4 exterior resonance for  $\mu=5.178 \times 10^{-5}$ . All the results are referred to the rotating frame of reference  $Oxyz$ . The eccentricity and the inclination vary along a family, but the semi-major axis is almost constant,  $a_{1/2} = 1.58740$ ,  $a_{2/3} = 1.31037$  and  $a_{3/4} = 1.21141$  (in non-dimensional units). It is worth noting that the *Kozai* resonance occurs when  $\omega$  librates around 0 (or  $\pi$ ) and  $\pi/2$  (or  $3\pi/2$ ). Then large oscillations of  $e$  and  $i$  are coupled with the motion of circulation/libration of  $\omega$ . So, the 3-D symmetric periodic orbits of Type 1 are associated with the *Kozai* resonance around  $\omega = \pi/2, 3\pi/2$  and the orbits of Type 2 are related with the above resonance around  $\omega=0, \pi$ .

### The 1/2 Resonance

There are two bifurcation points from the circular planar family  $II_{1/2}$  to 3-D orbits, at the eccentricities  $e = 0.059$  and  $e = 0.066$ , from which bifurcate the 3-D families  $A_1$  and  $A_2$ , respectively. Family  $A_1$  is of Type 1 and family  $A_2$  is of Type 2. In Figure 16a we show the family  $A_1$  of 3-D periodic orbits in the  $x_0 - h_0 - z_0$  space, which starts from the vertical critical orbit  $A_1 [e = 0.059, i = 0.0]$  with multiplicity 1 and terminates to a collision orbit with  $e = 0.986$  and  $i = 78.72^\circ$ , with multiplicity 2. Along the family  $A_1$  the multiplicity of 3-D periodic orbits changes from 1 to 2, from 2 to 3 and finally from 3 to 2. In Figures 16c and 16d we show the projections of this family to the  $x_0 - y_0$  and  $i - e$  planes. We observe that the eccentricity takes zero values at two points where the inclination is equal to  $27.5^\circ$  and  $98.4^\circ$ , respectively. The stability is shown in Figure 16d. The family  $A_1$  is unstable except for a small stable region between  $i = 55.7^\circ$  and  $i = 63.8^\circ$ . This means that we cannot have stable three dimensional motion of the small body in the 1/2 resonance, except for a small region with eccentricity close to  $e = 0.012$  and the inclination between  $i = 55.7^\circ$  and  $i = 63.8^\circ$ . Only in this region we can have stable librations around  $\omega = \pi/2$ , associated with the *Kozai* resonance.

In Figure 17a we present the family  $A_2$  (of Type 2) in the space  $(x_0, (dy/dt)_0, (dz/dt)_0)$ , which starts from the point  $A_2 [e = 0.066, i=0.0]$

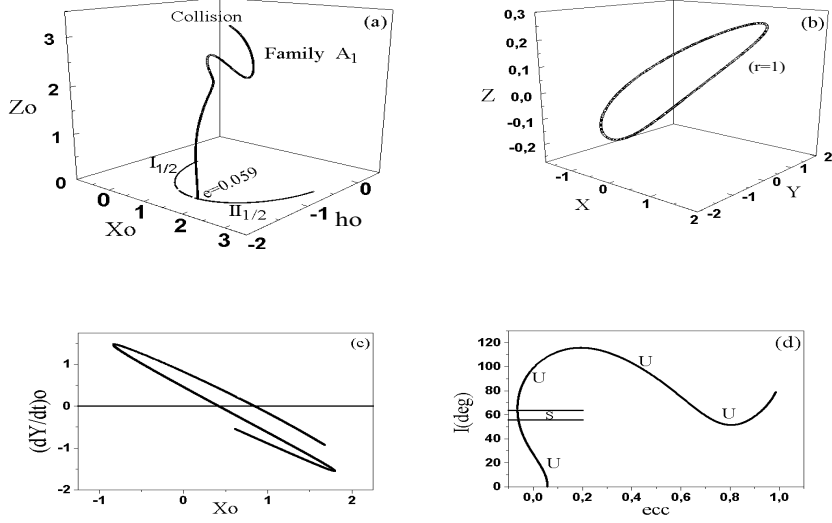


Figure 16. Resonance 1/2: (a) The family  $A_1$  in the  $x_0 - h_0 - z_0$  space, where  $h$  is the Jacobi-constant. (b) A 3-D symmetric periodic orbit of type 1 with multiplicity  $r = 1$ . (c) Projections of the family  $A_1$  to the  $x_0 - y_0$  plane and (d) to the  $i - e$  plane. The negative values of the eccentricity in Figure 16d stand for perihelion of the small body.

with multiplicity 1 and terminates at the point  $[e = 0.0, i = 180^\circ]$ , belonging to the retrograde family of planar periodic orbits (R) at the resonance 1/2 with multiplicity 3. In Figures 17c-d we give the projections of this family to the  $x_0 - z_0$  plane and to the  $i - e$  plane. The eccentricity takes zero values at two points along this family, with inclinations  $51.9^\circ$  and  $93^\circ$  respectively. Family  $A_2$  is unstable (Figure 17d), so no libration could exist around  $\omega=0$ .

### The 2/3 Resonance

Three vertical critical orbits along the family  $II_{2/3}$  of the planar problem were found from which bifurcate the 3-D families of periodic orbits. These points correspond to the eccentricities  $e_1 = 0.421$ ,  $e_2 = 0.450$  and  $e_3 = 0.968$ . From the first point there bifurcates the family  $B_1$  which is of type 1 and from the second and the third points there bifurcate two families, which in fact coincide, so we have one more family of 3-D periodic orbits,  $B_{23}$  which is of Type 2.

The family  $B_1$  of 3-D symmetric periodic orbits is presented in Figure 18a, in the  $x_0 - (dy/dt)_0 - z_0$  space. It starts from the vertical critical orbit  $B_1 [e = 0.421, i = 0.0]$  with multiplicity 1 and terminates to a collision orbit  $F_1 [e = 0.984, i = 70.18^\circ]$  with multiplicity 5. Along this family the eccentricity increases continuously up to a maximum value

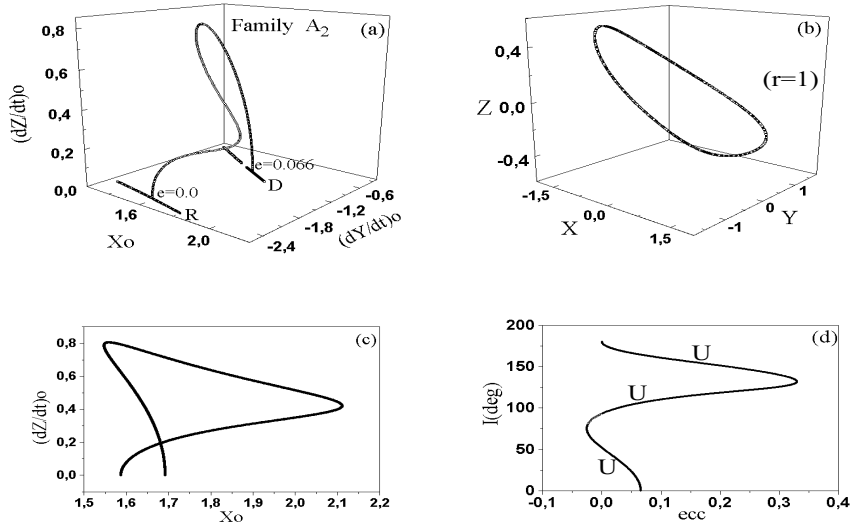


Figure 17. Resonance 1/2: (a) The family  $A_2$  in the  $x_0 - y_0 - z_0$  space,  $D$ :direct orbits,  $R$ :retrograde orbits. (b) A 3-D symmetric periodic orbit of type 2 with multiplicity  $r = 1$ . (c) Projection of the family  $A_2$  to the  $x - z$  plane, and (d) to the  $i - e$  plane. The negative values of the eccentricity denote the position of the small body at perihelion.

$e = 0.984$  at a collision orbit. The stability of this family is shown in Figure 18d. We note here that a large section of the family is stable and instability appears only at high eccentricities. So, we can have stable librations around  $\omega = \pi/2, 3\pi/2$  for quite large values of eccentricity and the inclination. This type of motion is associated with the Kozai resonance at the 2/3 resonance region (Morbidelli *et al*, 1995).

In figure 19a we present the family  $B_{23}$  (of Type 2) in the space  $(x_0 - e - i)$ , which starts from the point  $B_2 [e = 0.450, i = 0.0]$  of  $II_{2/3}$ , with multiplicity 1 and terminates at the point  $B_3 [e = 0.968, i = 0.0]$  of  $II_{2/3}$ , with multiplicity 5. In Figures 19c-19d we show the projections of the family  $B_{23}$  to the  $x_0 - (dz/dt)_0$  plane and to the  $i - e$  plane. Along this family the eccentricity increases continuously starting from large values ( $e = 0.45$ ) but the inclination starts from zero values, takes the maximum value at  $i_{max} = 79.03^\circ$  and finally terminates to zero values again. The stability is shown in Figure 19d. The family is unstable, so no libration could exist at the 2/3 resonance region, for non-zero inclination, around  $\omega = 0$ .

### The 3/4 Resonance

Five vertical critical orbits along the family  $II_{3/4}$  of the planar problem were found. These are:  $C_1 (e = 0.29)$ ,  $C_2 (e = 0.31)$ ,  $C_3 (e = 0.66)$ ,

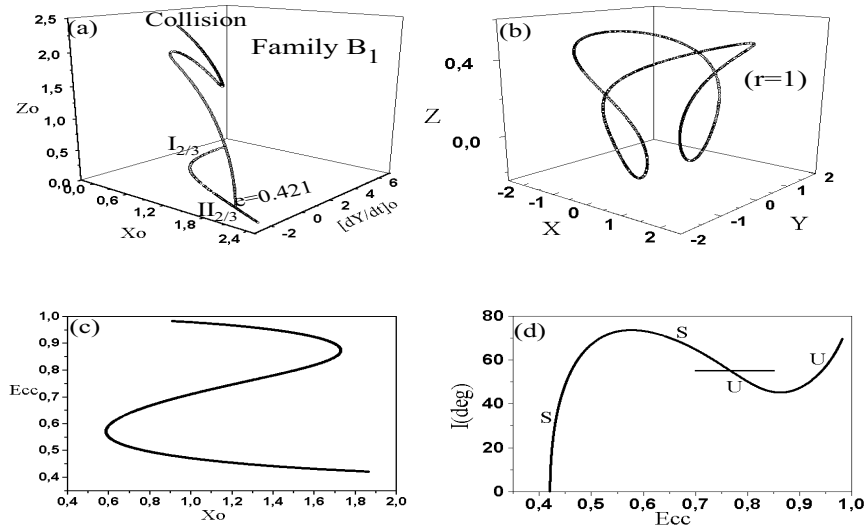


Figure 18. Resonance 2/3: (a) The family  $B_1$  in the  $x_0 - y_0 - z_0$  space. (b) A 3-D symmetric periodic orbit of type 1 with multiplicity  $r = 1$ . (c) Projection of this family to the  $x_0 - e$  plane and (d) to the  $i - e$  plane.

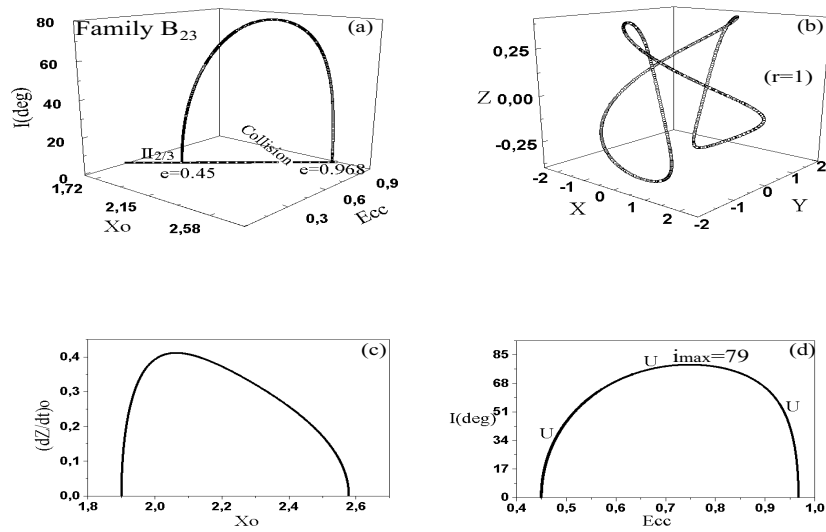


Figure 19. Resonance 2/3: (a) Family  $B_{23}$  in the space  $x_0 - e_0 - i_0$ . (b) A 3-D symmetric periodic orbit of type 2 with multiplicity  $r = 1$ . (c) Projection of this family to the  $x_0 - z_0$  plane and (d) to the  $e - i$  plane.

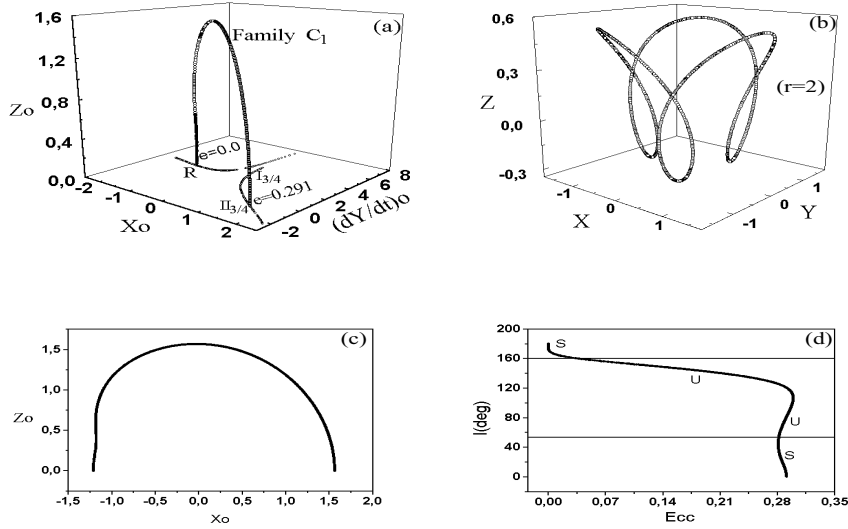


Figure 20. Resonance 3/4: (a) Family  $C_1$  in the  $x_0 - y_0 - z_0$  space,  $R$ : family of retrograde orbits. (b) A 3-D symmetric periodic orbit of type 1 with multiplicity 2. (c) Projection of this family to the  $x_0 - z_0$  plane and (d) to the  $e - i$  plane.

$C_4$  ( $e = 0.75$ ) and  $C_5$  ( $e = 0.77$ ). The families of 3-D symmetric periodic orbits which bifurcate from the points  $C_1$ ,  $C_3$ ,  $C_4$  have symmetry of Type 1 and the families which bifurcate from the points  $C_2$ ,  $C_5$  have symmetry of Type 2. As we shall see in the following, the families which bifurcate from the points  $C_2$  and  $C_5$  coincide.

In Figure 20a we present the family  $C_1$  of 3-D periodic orbits in the  $x_0 - (dy/dt)_0 - z_0$  space, which starts from the point  $C_1$  [ $e = 0.29$ ,  $i = 0.0$ ] with multiplicity 2 and terminates at the point [ $e = 0.0$ ,  $i = 180^\circ$ ], which belongs to the retrograde family of planar periodic orbits ( $R$ ) at the resonance 3/4, with multiplicity 7. The multiplicity of the 3-D orbits changes from 2 to 3, from 3 to 5 and finally from 5 to 7. In Figures 20c-20d we give the projections of the family  $C_1$  to the  $x_0 - z_0$  and to the  $i - e$  planes. Along this family the eccentricity decreases continuously and takes the minimum value ( $e_{min} = 0.0$ ) at the orbit  $G_1$ . The stability of this family is shown in Figure 20d. A large section of the family is unstable, from  $i = 54^\circ$  ( $e = 0.28$ ) to  $i = 160.5^\circ$  ( $e = 0.033$ ) and stability appears at low to moderate values of eccentricity. So, we can have stable librations around  $\omega = \pi/2$ , for small values of the eccentricity and the inclination. This type of motion is associated with the *Kozai* resonance at the 3/4 resonance region.

In Figure 21a we show the family  $C_{25}$  in the space  $(x_0 - e_0 - i_0)$ , which starts from the point  $C_2$  [ $e = 0.31$ ,  $i = 0.0$ ] with multiplicity 2 and terminates at the point  $C_5$  [ $e = 0.77$ ,  $i = 0.0$ ] with multiplicity

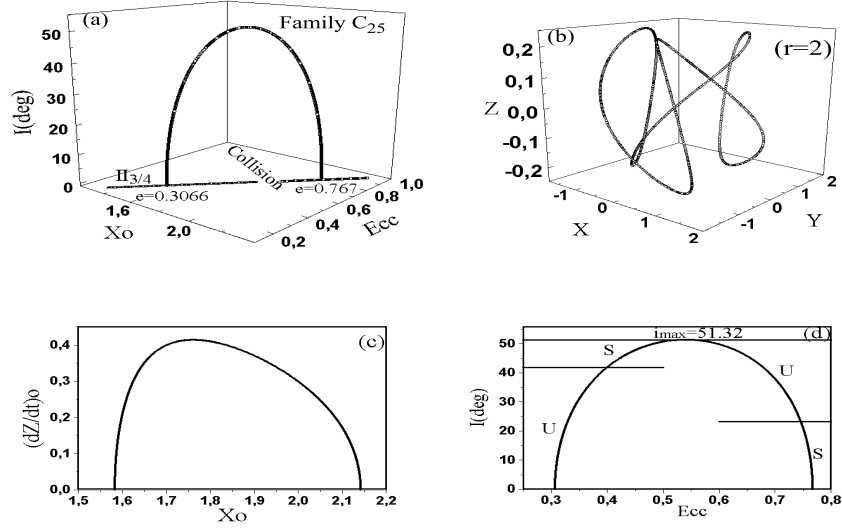


Figure 21. Resonance 3/4: (a) Family  $C_{25}$  in the space  $x_0 - e_0 - i_0$ . The gap along the family  $II_{3/4}$  of the planar problem is that of Figure 5b. (b) A 3-D symmetric periodic orbit of type 2 with multiplicity 2. (c) Projection of the family to the  $e - i$  plane and (d) to the  $x_0 - e_0$  plane.

4. In Figures 21c-d we show the projections of the family  $C_{25}$  to the  $x_0 - (dz/dt)_0$  and  $x_0 - e_0$  planes. Along this family the eccentricity increases continuously but the inclination starts from zero values, takes the maximum value at  $i_{max} = 51.33^\circ$  and ends again to zero values. The stability is shown in Figure 21d. Two stable areas appear along the family: one between  $e = 0.4$  ( $i = 41.9^\circ$ ) and  $e = 0.54$  ( $i = 51.3^\circ$ ) and the other between  $e = 0.75$  ( $i = 21.2^\circ$ ) and  $e = 0.77$  ( $i = 0.0^\circ$ ). So, we can have stable librations around  $\omega = 0, \pi$  at these regions of  $e$  and  $i$ .

In Figure 22a we present the family  $C_3$  of 3D-periodic orbits. It starts from  $C_3$  [ $e = 0.66, i = 0.0$ ] with multiplicity 4 and terminates at the point  $G_3$  [ $e = 0.35, i = 180^\circ$ ] which belongs to the retrograde family of planar periodic orbits ( $R$ ) at the resonance 3/4, mentioned above, with multiplicity 7. Along the family  $C_3$  the multiplicity of the 3-D orbits changes from 4 to 2, then from 2 to 3, to 5 and finally to 7. The projections of this family on the planes  $x_0 - z_0$  and  $i - e$  are given in Figures 22c-22d, respectively. Along this family the eccentricity decreases continuously and finally takes the minimum value ( $e_{min} = 0.35$ ) at the point  $G_3$ . The stability of the family  $C_3$  is presented at Figure 23d. The family  $C_3$  is unstable except for two regions: one is located between  $i = 7^\circ$  ( $e = 0.655$ ) and  $i = 10^\circ$  ( $e = 0.650$ ) and the region between  $i = 120^\circ$  ( $e = 0.44$ ) and  $i = 180^\circ$  ( $e = 0.35$ ). So, stable librations around  $\omega = \pi/2$  can exist at these regions of  $e$  and  $i$ .

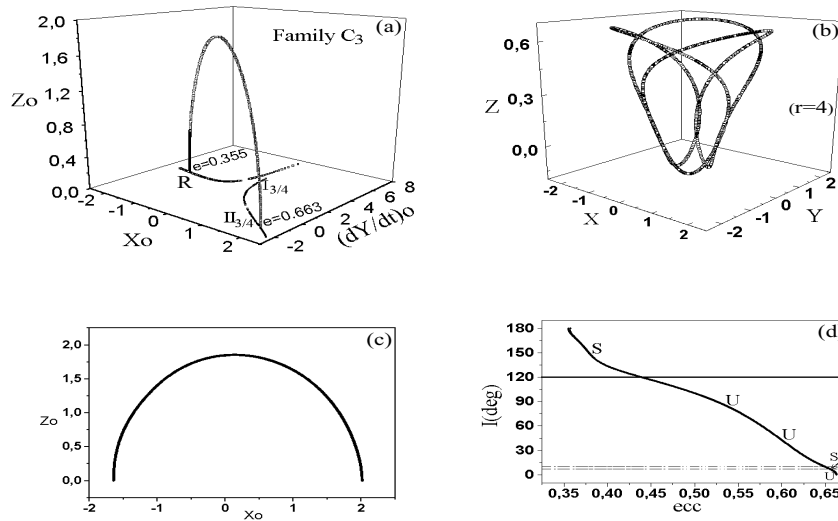


Figure 22. Resonance 3/4: (a) Family  $C_3$  in the  $x_0 - y_0 - z_0$  space. ( $I_{3/4}$ ,  $II_{3/4}$ : families of direct orbits described in Figure 5b,  $R$ : family of retrograde orbits). (b) A 3-D symmetric periodic orbit of type 1 with multiplicity 4. (c) Projection of the family  $C_3$  to the plane  $x_0 - z_0$  and (d) to the  $i - e$  plane.

Finally, the family  $C_4$  of 3D-periodic orbits is shown in the Figure 23a. It starts from  $C_4$  [ $e = 0.75$ ,  $i = 0.0$ ] with multiplicity 4 and terminates at a collision orbit  $G_4$  [ $e = 0.97$ ,  $i = 65.96^\circ$ ]. The multiplicity of 3-D periodic orbits remains the same along the family  $C_4$  and no maximum appears. The eccentricity increases along this family starting from high values; the inclination increases, starting from zero values. The stability is presented in 23d. Family  $C_4$  is unstable up to  $i = 14.4^\circ$  ( $e = 0.795$ ) and then becomes stable. We note that a large section of the family is stable, and instability appears only at high eccentricities but small inclinations. So, we can have stable librations around  $\omega = \pi/2$ , for quite large values of the eccentricity and the inclination. This type of motion is associated with the Kozai resonance at the 3/4 resonance region.

## 6. The 3-D Elliptic Restricted 3-Body Problem

As far as the 3-D elliptic restricted three-body problem is concerned, we remark here that families of periodic orbits of the 3-D elliptic restricted three-body problem, with the eccentricity of Neptune as a parameter, bifurcate from the families of the 3-D circular problem mentioned above. The bifurcation can take place only at those orbits of the circular problem whose period is equal to  $\pi$  or  $2\pi$  or a multiple

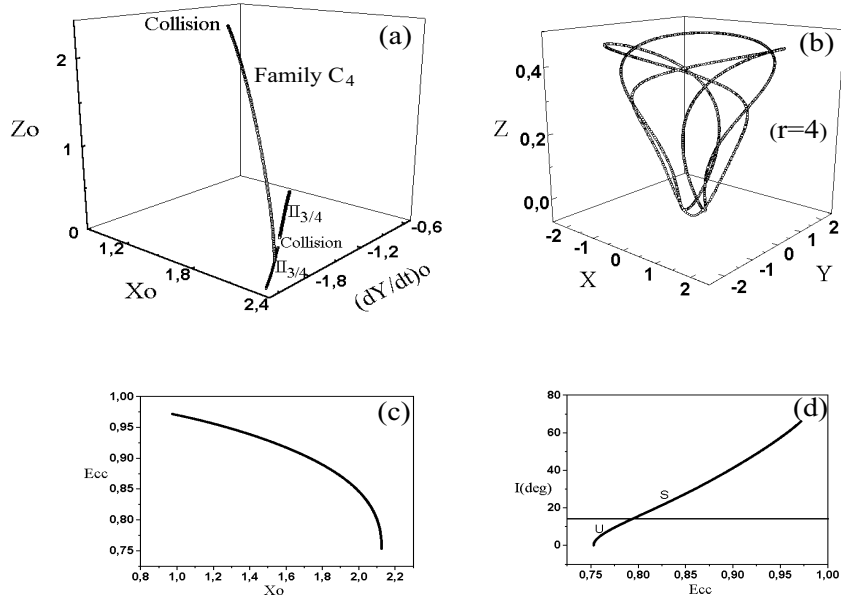


Figure 23. Resonance 3/4: (a) Family  $C_4$  in the  $x_0 - y_0 - z_0$  space. The gap along the family  $II_{3/4}$  is that of Figure 5b. (b) A 3-D periodic orbit of type 1 with multiplicity 4. (c) Projection of the family  $C_4$  to the plane  $x_0 - e_0$  and (d) to the plane  $e - i$ .

of it. Examining the variation of period  $T$  along each family of the 3-D circular restricted 3-body problem, we found that there exist periodic orbits along the families  $A_1$ ,  $A_2$  at the resonance 1/2, whose period is equal to  $4\pi$  and along the families  $C_1$ ,  $C_3$  at the resonance 3/4 with period exactly equal to  $8\pi$ . There are not any periodic orbits of the 3-D circular problem at the resonance 2/3 with period equal to  $6\pi$ . The results are summarized in Table 3.

TABLE 3  
*Bifurcation from the 3-D circular to the 3-D elliptic problem*

Resonance	$a$ (in A.U.)	Period	Family	Bifurcation Points
1/2	47.777	$4\pi$	$A_1$	$e=0.05, i=80.02^\circ$
1/2	47.777	$4\pi$	$A_1$	$e=0.27, i=113.80^\circ$
1/2	47.777	$4\pi$	$A_2$	$e=0.04, i=101.66^\circ$
3/4	36.415	$8\pi$	$C_1$	$e=0.29, i=75.84^\circ$
3/4	36.415	$8\pi$	$C_3$	$e=0.52, i=93.74^\circ$

Another way to find periodic orbits that give bifurcation to the 3-D elliptic restricted three-body problem is to study the vertical stability of periodic orbits of the planar elliptic problem. Following the same methodology as in the circular case, we computed the vertical stability of the planar elliptic problem. In the case of 1/2 resonance, the computations revealed that there exists one vertical critical orbit on the family  $E_{1p}^{1/2}$  at  $e = 0.218$ ,  $e_N = 0.474$ . We note here that family  $E_{1p}^{1/2}$  is vertically stable for  $e_N < 0.474$  and becomes vertically unstable for  $e_N > 0.474$ . This bifurcation however is of no interest for the study of the Edgeworth-Kuiper belt, because the value of  $e_N$  is very high.

The families  $E_{1a}^{1/2}$ ,  $E_{2p}^{1/2}$  and  $E_{2a}^{1/2}$  of the 1/2 resonance, the families  $E_p^{2/3}$  and  $E_a^{2/3}$  of the 2/3 resonance and the families  $E_p^{3/4}$  and  $E_a^{3/4}$  of the 3/4 resonance are all vertically stable. So, no vertical critical orbits exist and consequently these families cannot give bifurcation to the 3-D elliptic periodic orbits.

## 7. Discussion

The stability and the evolution of a small body in the Edgeworth-Kuiper belt is determined by the topology of the phase space. This depends on the model we use in our study. The complete problem involves all the major planets, so we have a system with many degrees of freedom. This makes it very difficult to obtain a view of the phase space and the only way to study the evolution of a small body is to use numerical integrations. In this case, the selection of the initial conditions is a major problem. A grid in the whole phase space involves too many initial conditions, and consequently too much computing time, which is costly, even with the present computers. The most important problem however is the study of the vast amount of output that we get in this way. So, there is the danger to be lost in unnecessary details and miss the main properties of the phase space.

A different approach is to simplify the physical problem, by considering the averaged Hamiltonian. In this way the problem becomes manageable (in fact by generating ignorable coordinates by a series of canonical transformations), but at the expense of losing degrees of freedom. This is theoretically correct if the system is integrable, or, approximately, if we are in an ordered region of the phase space. Since however the problem is non integrable, chaotic regions are expected and consequently the perturbation series in the averaged model are not convergent. So, important information may be lost.

The selection of the model which we will use is a crucial point. In the present study we use Neptune as the main perturbing body. Although

the other major planets affect also the evolution, the topology of the phase space, as obtained by the simpler model *Sun - Neptune - small body*, will give us useful information for the evolution of the small body. In fact, the chaotic regions in this model will remain chaotic when the effect of the other planets is included. On the other hand, stable regions of the simple model are not expected to become chaotic, if we are not close to secular resonances.

The complete model in the present study is the three dimensional elliptic three body problem, with the Sun and Neptune as primaries and Neptune in a fixed elliptic orbit. This is a non autonomous system with three degrees of freedom, and is already quite complicated. The simplest model is to consider the orbit of Neptune circular and study planar orbits (circular planar model). This is a simple autonomous system with two degrees of freedom, whose phase space can be easily studied (note that the Poincaré map on a surface of section is two dimensional). This model is not realistic, because the ellipticity of the orbit of Neptune and the inclination of the orbit of the small body introduce additional degrees of freedom, which affect critically the topology of the phase space.

Malhotra(1996) has made a systematic study of the topology of the phase space in the circular planar model and several resonances were included. Both regular zones appear, where we have stable librations and also chaotic zones, due to overlap of resonances, where diffusion can take place. In the present study we started with this simple model and we extended the study to the complete model.

The basic idea in the present work is based on the fact that the topology of the phase space, in any model, is shaped by the position and the stability character of the periodic orbits. It is in the vicinity of a stable periodic orbit that librations are expected. On the contrary, it is close to an unstable periodic orbit that chaotic motion appears. In addition, the closeness of the families of resonant periodic orbits is an indication of the extent of the stable libration and the generation of chaotic regions due to resonance overlap. Furthermore, the absence of low order resonant periodic orbits implies a smooth phase space, with ordered motion only. For this reason, instead of being lost in a vast set of initial conditions, the periodic orbits should be used as the basic tool to select the initial conditions. In this way, no important feature of the phase space can be lost.

We started the study with the simplest model, the circular planar model, as the starting point. The topology of the phase space of the circular planar model is shown in Figure 12, where the Poicaré maps for different energy levels are computed (see also Malhotra, 1966). The guide for the selection of the energy levels was provided by the Figure

1 (and Figures 3-5 in more detail). The relation between the families of periodic orbits and the appearance of the corresponding fixed points on the maps is clear. In fact, a crude idea of the topology of the phase space, as shown in Figure 12, could be obtained from Figures 1,3-5 alone.

From Figure 12 we note that there are stable libration zones in all basic first order resonances, namely  $1/2$ ,  $2/3$  and  $3/4$ , corresponding to the stable fixed points/periodic orbits. As the energy level increases, more and more resonances appear and consequently the stable libration zones shrink, and chaotic regions appear, due to resonance overlap. If we restricted ourselves to the circular planar model, we would come to the conclusion that the  $1/2$  resonance should be the one with the larger population, because this resonance is not very close to the other resonances and consequently large libration zones exist.

The above picture for the topology of the phase space close to the  $1/2$ ,  $2/3$  and  $3/4$  resonances changes drastically when we go to the more realistic model, by considering the inclination of the orbit of the small body and the ellipticity of the orbit of Neptune.

#### elliptic planar model

- In section 4 it is found that in the  $1/2$  resonance the topology of the phase space in the elliptic planar model is shaped by two pairs of families of *unstable* periodic orbits, one of them with very small eccentricities ( $e = 0.07$ ) of the small body, which are close to each other. This means that there exist two unstable periodic orbits, close to each other, in the system Sun - Neptune - small body ( $e_N = 0.011$ ). Consequently, large chaotic regions appear as the eccentricity of Neptune is introduced, for small values of  $e$ , and this changes dramatically the picture we had from the circular model.
- In the  $2/3$  resonance we found that no periodic orbits exist for small values of the eccentricity. A pair of unstable families exists only at high values of the eccentricity ( $e = 0.47$ ), and consequently two unstable periodic orbits exist for  $e_N = 0.011$ . This means that the phase space is smooth, in the elliptic model, for small values of the eccentricity.
- In the  $3/4$  resonance a pair of unstable periodic orbits exists, at eccentricities  $e = 0.33$  and consequently two unstable periodic orbits exist for  $e_N = 0.011$ . For smaller eccentricities the phase space is smooth, but in the circular planar model this region is quite chaotic and the libration zone is quite small (Figure 12).

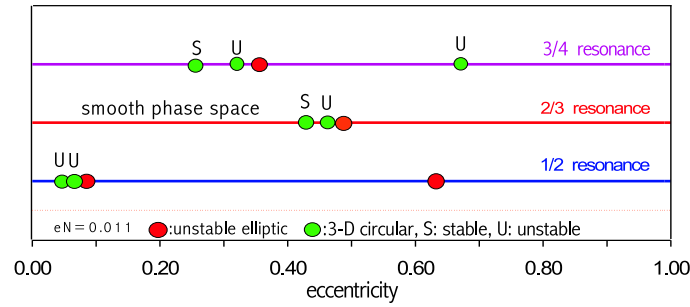


Figure 24. Bifurcations from the circular planar model to the elliptic planar model and to the circular 3-D model, and stability.

### *3-D circular model*

- In section 5 it is found that in the  $1/2$  resonance there exist two families of unstable periodic orbits for very small values of the eccentricity ( $e = 0.07$ ) and values of the inclination smaller than  $i = 60^\circ$ .
- In the  $2/3$  resonance a stable family exists for eccentricities close to  $e = 0.42$  and inclinations which can reach high values, up to  $i = 60^\circ$ . This family of periodic orbits is of type 1, so the stable librations in its vicinity are around  $\omega = \pi/2$  or  $\omega = 3\pi/2$ .
- The topology of the phase space of the 3-D model at the  $3/4$  resonance appears very complicated. Four families of periodic orbits exist, all with  $e > 0.29$ . Only one of them, with eccentricity close to  $e = 0.29$  and values of the inclination  $0 < i = 40^\circ$  is stable. This corresponds to stable librations around  $\Omega = \pi/2$ . Stable regions appear also on some of the other families, but for large values of both  $e$  and  $i$ .

From all the above results, which are summarized in Figure 24, we note that the only resonance in which stable regions exist is the  $2/3$  resonance: In the region  $0 < e < 0.42$  there are not periodic orbits in the 3-D case, so the phase space is smooth. This property of the phase space is not destroyed when the ellipticity of the orbit of Neptune is introduced, because up to these values of  $e$  the phase space is smooth in the elliptic model (the two unstable periodic orbits for  $e_N = 0.011$  appear for  $e > 0.47$ ). This means that we can have stable librations at these values of the eccentricity and the inclination, which are around  $\omega = \pi/2, 3\pi/2$ . This type of libration is associated with the Kozai resonance.

In the  $1/2$  resonance we have an unstable region in the elliptic model, for small values of the eccentricity. This means that we cannot have trapping at this resonance, for small values of  $e$ . In addition, unstable motion appears in the 3-D circular model for small values of the eccentricity. So, we cannot have trapping in this region. However, the region  $e < 0.07$  and  $i > 0$  does not contain any periodic orbits. This implies that the phase space is smooth and we can have bodies in this region, in a semistable motion (stable chaos).

In the  $3/4$  resonance the instability starts from the circular planar model. However, the phase space in the elliptic model and the 3-D model appears as smooth, for eccentricities smaller than  $e = 0.30$  and inclinations smaller than  $i = 40^\circ$  (because in this region there are not periodic orbits in the elliptic model, and there exist stable periodic orbits in the 3-D model).

The above conclusions are based on the study of the bifurcation points to families of periodic orbits of the circular 3-D problem or the planar elliptic problem. This study made clear the importance of the position and the stability character of these bifurcation points. This phenomenon is also evident in the asteroid belt, as shown by Tsiganis et. al (2001). It is also made clear that the topology of the simplest model, the circular planar model, does not represent the real model.

The above results are in accordance with the observations, that the  $2/3$  resonance region is populated with many objects and the other resonances are almost empty.

The above analysis was based on the exploration of the phase space of the elliptic three dimensional restricted three body problem, by making use of the position and the stability character of the low order resonant periodic orbits of the system. A more detailed analysis, based on exact numerical integrations and taking into account all major planets, can be made using as initial conditions those regions of the phase space (of the Sun - Neptune - small object system) which are close to stable periodic motion, or far from periodic motion, to detect stable librations. Or using initial conditions close to unstable periodic orbits, or regions where many resonances exist close to each other, to detect chaotic regions and study the diffusion of a small object and the mechanism it may become a short period comet.

### Acknowledgements

Thomas A. Kotoulas is financially supported by the Hellenic Scholarship Foundation (I.K.Y.).

## References

- Beaugé, C.:1994, *Celest. Mech. and Dyn. Astron.* **60**, 225-248.
- Broucke, R.A.:1969, *Stability of the Periodic Orbits in the Restricted Three Body Problem*, *AIAA* **7**, 1003-1009.
- Colombo, G., Franklin, F.A., Munford, C.M.:1968, *Astron.J.***73**,111-123.
- Duncan, M.J., Levison, H.F. and Budd, S.M. (1995): *The dynamical structure of the Kuiper Belt*, *Astron. J.* **110** (6), December 1995, 3073-3081.
- Gallardo T. and Ferraz-Mello, S.:1998, *Dynamics of the 2/3 exterior resonance with Neptune*, *Planet Space Sci.*, Vol. 46, No. 8, 945-965.
- Hadjidemetriou, J.D.:1975, *Celes.Mech.* **12**, 155-174.
- Hadjidemetriou, J.D.:1975, *The Stability of periodic orbits in the three-body problem*, *Celes.Mech.* **12**, 255-276.
- Hadjidemetriou, J.D. (1988): *Periodic Orbits of the Planetary type and their stability*, *Celes.Mech.* **43**, 371-390.
- Hadjidemetriou, J.D. (1993): *Resonant motion in the restricted three body problem*, *Cel.Mech and Dyn. Astr.* **56**, 201-219.
- Hénon, M: 1965, *Ann. Astrophys.* **28**, 992.
- Hénon, M. (1969): *Numerical Exploration of the Restricted Problem*, *Astron.Astrophys.* **1**, 223-238.
- Hénon, M.(1973): *Vertical Stability of Periodic Orbits in the Restricted Problem*, *Astron.Astrophys.***28**, 415-426.
- Jewitt, D., Luu, J.X. and Trujillo, C. (1998): *Large Kuiper Belt Objects: The Mauna Kea 8K CCD Survey*, *Astron. J.* **115**, May 1998, 2125-2135.
- Jewitt, D. (1999): *Kuiper Belt Objects*, *Annu. Rev. Planet. Sci.* **27**, 287-312.
- Jewitt, D. and Luu, J.X. (2000): *Physical Nature of the Kuiper Belt. Protostars and Planets IV*, Vince Mannings (ed.), Univ. Az. press, pp.1201-1229.
- Levinson, H.F. and Duncan, M.J.:1994, *Icarus* **108**, 18-36.
- Levinson, H.F. and Stern, S.A.:1995, *Icarus* **116**, 315-339.
- Lichtenberg, A.J. and Leibermann, M.A.:1983, *Regular and Stochastic Motion*, Springer-Verlag.
- Malhotra, R.:1996, *The Phase Space near Neptune Resonances in the Kuiper Belt*, *Astron. J.* **111** (1), January 1996, 504-516.
- Maran, M.D. and Williams, I.P. (2000): *The evolution of bodies orbiting in the trans-Neptunian region on to intermediate-type orbits*, *Mon. Not. R. Astron. Soc.* **318**, 482-492.
- Morbidelli, A., Thomas, F. and Moons, M.:1995, *The resonant Structure of the Kuiper Belt and the Dynamics of the First Five Trans-Neptunian Objects*, *Icarus* **118**, 322-340.
- Morbidelli, A.:1999, *An overview on the Kuiper Belt and on the Origin of Jupiter-Family Comets*, *Cel.Mech. and Dyn.Astr.* **72**, 129-156.
- Nesvorný, D. and Roig, F. (2000): *Mean Motion Resonances in the Trans-neptunian Region, I. The 2/3 Resonance with Neptune*, *Icarus* **48**, 282-300.
- Roy, A.E.:1982, *Orbital Motion*, Adam Hilger, (2<sup>nd</sup> ed.).
- Thomas, F. and Morbidelli, A.:1996, *The Kozai Resonance in the Outer Solar System and the Dynamics of the Long-Period Comets*, *Cel.Mech and Dyn.Astr.* **64**, 209-229.
- Tsiganis, K., Varvoglis, H., and Hadjidemetriou, JD. 2001: *Stable chaos in high-order Jovian resonances*, *Icarus* (to appear).
- Yu, Q. and Tremaine, S. (1999): *The Dynamics of Plutinos*, *Astron. J.* **118**, 1873-1881.